How serious is the nonlinear effect on traveltime delays predicted by sensitivity kernels

Wenjun Xu[**] and Xiao-Bi Xie[*],
**Institute of Geophysics and Planetary Physics, University of California, Santa Cruz, CA 95064*
[*]College of Earth and Marine Sciences, Tongji University, Shanghai, China

Summary

Sensitivity kernels are used in travel-time tomography and waveform inversion for its obvious advantages in matching wave-motion theory rather than ray theory. However, there still remain some concerns regarding its accuracy and when the small-perturbation theory will break down. We investigate these questions using numerical simulations. Sensitivity kernels calculated in the background model and based on the linear scattering theory are used to predict the traveltime delay caused by the velocity perturbations. On the other hand, the traveltime differences between the background and the perturbed velocity models are directly calculated from the synthetic seismograms generated by the finite-difference method. The predicted traveltime delays are compared to these direct measurements and the results are used to judge the accuracy of the linear theory. Velocity models with perturbations of different scales or different perturbation values are used to conduct the tests. Our results show that extending the scale or increasing the amplitude of the velocity perturbations or both can affect the precision of the traveltime sensitivity kernel. These factors also complicate waveforms of synthetic seismograms as well as the shape of the sensitivity kernels in the perturbed velocity model. Nevertheless, within a large range of velocity perturbations, the sensitivity kernels based on linear theory still give reasonably accurate traveltime delay, indicating the linearization plus iteration method is still effective under reasonably large velocity perturbations.

Introduction

Sensitivity (Fréchet) kernels have been widely studied since the ray-theory-based traveltime calculation is not enough to depict or simulate the real wave phenomena. The problem how to break through the high-frequency limitation of ray theory has always been a hot issue. So, using sensitivity kernels to compute the time delays or amplitude changes attracts the sight of the researchers. Traveltime and amplitude sensitivity kernels have been discussed and optimized under paraxial approximation (by Coates , 1990; Woodward, 1992; Marquering, 1998, 1999; Dahlen, 2000; Xie, 2008). Liu et al. (2008) used sensitivity kernels to compute the transmitted wave traveltime. And Yue et al. (2006) discussed the numerical precision and validity of paraxial approximation using analytical expressions.

When using sensitivity kernels to compute the time delays, attentions must be taken for validation of preconditions and precision of finite-frequency sensitivity kernel calculation. Here, we discuss the linear relationship of kernel integral when under Born approximation and the nonlinearity beyond theory of small perturbation.

To get a comprehensive understanding of wave-theory tomography, we start from the kernel integral equation. Then we discuss how the kernels are sensitive to the velocity perturbation by numerical simulation and how the the kernel integral acts when the assumption of small perturbation fails to hold any more.

Theoretical Overview

Under the finite-frequency sensitivity theory, the difference between traveltimes from a perturbed velocity model and the background velocity model can be calculated as (e.g., Woodward, 1992)

$$\delta t(\mathbf{r}_g, \mathbf{r}_s) = \int m(\mathbf{r}')K(\mathbf{r}', \mathbf{r}_g, \mathbf{r}_s)\, dV, \qquad (1)$$

where $\delta t(\mathbf{r}_g, \mathbf{r}_s)$is the broadband traveltime delay, $\mathbf{r}_s$ and $\mathbf{r}_g$ are locations of the source and receiver, $m(\mathbf{r}') = \delta v(\mathbf{r})/v_0(\mathbf{r})$ is the velocity perturbation, $K(\mathbf{r}', \mathbf{r}_g, \mathbf{r}_s)$ is the broadband sensitivity kernel which can be obtained from single frequency sensitivity kernels

$$K(\mathbf{r}', \mathbf{r}_g, \mathbf{r}_s) = \int \frac{W(\omega)}{\omega} K_f(\mathbf{r}', \mathbf{r}_g, \mathbf{r}_s, \omega) d\omega, \qquad (2)$$

where $W(\omega)$ is a weighting function (Xie and Yang, 2008a). Based on Born and Rytov approximations, the single frequency kernel $K_f(\mathbf{r}', \mathbf{r}_g, \mathbf{r}_s, \omega)$ can be calculated as

$$K_f(\mathbf{r}', \mathbf{r}_g, \mathbf{r}_s, \omega) = \mathrm{imag}(2k_0^2 \frac{G(\mathbf{r}', \mathbf{r}_s, \omega) G(\mathbf{r}', \mathbf{r}_g, \omega)}{G(\mathbf{r}_g, \mathbf{r}_s, \omega)}), \qquad (3)$$

where $G(\mathbf{r}', \mathbf{r}_s, \omega)$, $G(\mathbf{r}', \mathbf{r}_g, \omega)$ and $G(\mathbf{r}_g, \mathbf{r}_s, \omega)$ are Green's functions from the source to the scatters, from the receiver to the scatters and from source to receiver, respectively. They are all calculated in the background velocity. Equation (3) is obtained based on linear scattering theory by assuming the perturbations are small. In tomography inversions, equations (1) to (3) are frequently used to predict the travel time delays due to velocity perturbations. In the practice of applied seismology, the velocity perturbations are not necessarily small values. Theoretically, the change of velocity model also modifies the sensitivity kernel, i.e., the problem is actually nonlinear. How big the velocity perturbation that the linear sensitivity

How serious is the nonlinear effect on traveltime delays predicted by sensitivity kernels

kernel built in the reference model can handle is crucial for safely applying these equations in tomography and velocity model building. We explore this problem using numerical simulations. The traveltime delays predicted by sensitivity kernels are compared to traveltime directly measured from finite-difference generated synthetic seismograms and the results are used to judge the validity of the linear theory.

Numerical Tests

We use the same velocity models to calculate sensitivity kernels and generate synthetic seismograms. The 2D velocity model is 6000 m by 6000 m with a 20 m grid space. The length of the synthetic seismogram is 1.84 s with a time interval of 3.2 ms. A Ricker wavelet with a center frequency of 7.5 Hz is used for both the finite-difference calculations and generating sensitivity kernels. The background velocity is 2000 m/s. The source and receiver are separated by 3000 m. For investigating the effect of velocity models on traveltime calculations from both sensitivity kernel and finite-difference simulations, velocity perturbations with different patch sizes and perturbation amplitudes are added to the background model.

Traveltime sensitivity kernels in constant velocity model

As a comparison, we first use equations (2) and (3) to generate the traveltime sensitivity kernel in a homogeneous background velocity model. Illustrated in Figs (1) is the 7.5 Hz single-frequency sensitivity kernel, which is symmetric to the geometrical ray linking the source to receiver. Shown in Fig. 2 is the broadband sensitivity kernel. We see that the amplitudes of different frequency components are different. The higher frequency component has the larger amplitude and is narrower for its first Fresnel zone. When summing all the frequency components, the kernel performs as the higher-frequency component does. Beyond the first Fresnel zone, energy of kernel reduces to zero due to interference.

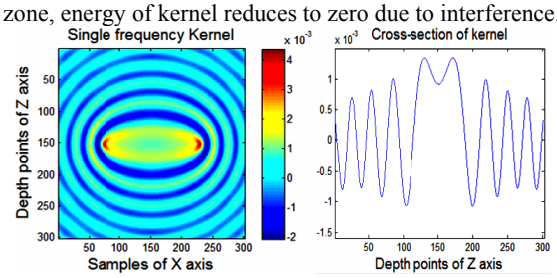

(a) (b)

Fig. 1. Single-frequency sensitivity kernel for a 2D homogenous medium, with (a) the sensitivity kernel; and (b) its transverse cross section.

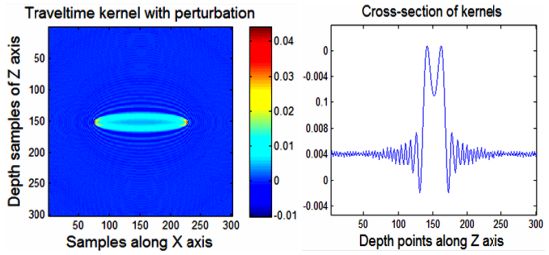

(a) (b)

Fig. 2. Broadband sensitivity kernel for the 2D homogenous medium, with (a) the broadband traveltime sensitivity kernel; and (b) the transverse cross-section of the sensitivity kernel.

Traveltime sensitivity kernels in a perturbed velocity model

To investigate how velocity perturbations can affect the shape of sensitivity kernels, we add a Gaussian distributed circular velocity perturbation patch in the model and move its location to test its effect on the kernel calculation. The circular patch has a radius of 600 m and a positive velocity perturbation of 40%. The sensitivity kernel in the perturbed model is shown in Fig. 3(b). Also indicated in the figure is the location of the perturbation patch. As a comparison, the sensitivity kernel in the background model is presented in Fig. 3(a). We see that the higher-velocity perturbation provide a faster shortcut and attracts the energy passing through it. This makes the kernel appear fatter. Shown in Fig. 4(a), when the higher-velocity perturbation is located close to the geometrical ray, the sensitivity kernel becomes thinner. On the contrary, if the velocity perturbation is negative, it will prevent the wave from passing through it. If it sits close to the geometric ray, the kernel will become fatter. If it sits outside of the kernel, it will make the kernel thinner.

For the above mentioned cases, the synthetic seismograms generated by finite-difference method also show different behaviors both in time-delay and amplitude. The waveform shown in Fig. 5(a) corresponds to the kernel shown in Fig. 3(b). The blue trace is calculated from the background model and the green trace is from the perturbed velocity model. In this case, the travel time is delayed while the amplitude is increased. The waveform shown in Fig. 5(b) corresponds to the kernel shown in Fig. 4(a). In this case, the travel time is advance while the amplitude is decreased.

Comparison between the Traveltime Delays from the Finite-Difference Calculation and Predicted by the Sensitivity Kernel

In this part, we design two types of models. First, we use velocity perturbations that have the same patch size but

How serious is the nonlinear effect on traveltime delays predicted by sensitivity kernels

with different perturbation values to calculate sensitive kernels and synthetic seismograms. The perturbations are ranging between 5%, 10%, 20%, 40%, 60%, 100% and 200% , and the patch has a radius of 600 m. For sensitivity kernels, the time delay is calculated using equation (1), and for finite-difference generated synthetic seismograms, the time delay is directly measured form the corss-correlation between waveforms. The results are compared in Fig. 6, in which the horizontal coordinate is for traveltime delays measured from the synthetic seismograms, and the vertical coordinate is for traveltime delays predicted by using the sensitivity kernels. The red square is the time-delay for 5% perturbation, green square is for 10% perturbation, yellow square is for 20% perturbation, blue square is for 40% perturbation, black square is for 60% perturbation, sky-blue square is for 80% perturbation, pink square is for 100% perturbation, and the solid red, green, yellow, blue, and black circles are for 120, 140, 160, 180, 200% perturbations. The black dashed line with the unit slope stands for the ideal linearity. We see that when the velocity perturbation is less than 60%, we get a nice linear relationship between the time delays from kernel integral and cross-correlation. For velocities beyond 60%, the relationship between the two time delays is no longer strictly straight, indicating the nonlinear effect from larger velocity perturbations. In this situation, the Born approximation becomes less accurate.

In the second model, we fix the perturbation at 40%, 60%, 100%, and 150%, but expand the size of the circular perturbation patch from 600 m, to 800, 1000, 1200, 1400, 1600, and 1800 m. Then measure the delay time of each instance. The results are shown in Fig. 7. The velocity perturbations are grouped using line colors, where the blue line is for 40%, green line is for 60%, sky-blue line is for 100% and pink line is for 150%. The sizes of the perturbation patch are color coded, where the red points are for 600 m patch, green points are for 800 m patch, yellow points are for 1000 m patch, blue points are for 1200 m, black points are for 1400 m, sky-blue points are for 1600 m, and the pink points are for 1800 m. The black dashed line stands for the ideal linearity. We see that when the perturbation has a small size or a small value, the time-delay by kernel integral shows good consistent linear relationship with the real time delay measured by correlation. However, once the perturbation is bigger of size or of value, the linearity is deterited.

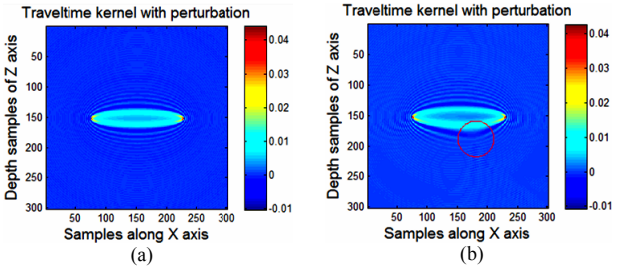

(a) (b)

Fig.3. Sensitivity kernels for the 2D homogenous model and for the model with a small higher-velocity body: (a) constant-medium traveltime sensitivity kernel; (b) sensitivity kernel when a velocity perturbation exists in the lower part of the model.

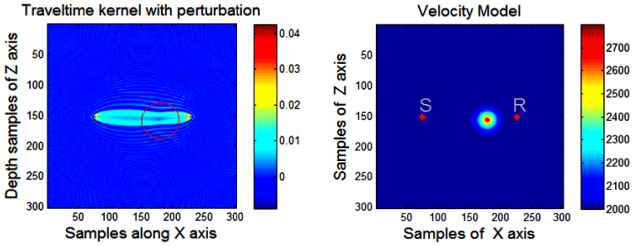

(a) (b)

Fig.4. Similar to Fig. 3 except the perturbation is located close to the geometrical ray: (a) the sensitivity kernel; (b) the model with the circular velocity perturbation.

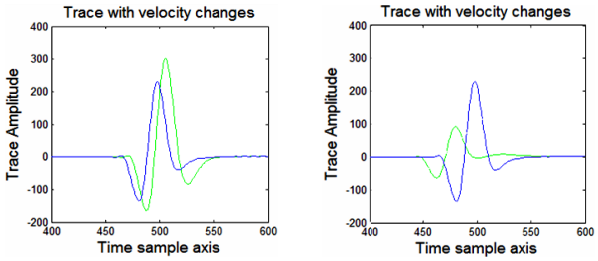

(a) (a)

Fig.5. Traces of synthetic seismograms. The blue traces are calculated in the background model and the green traces are calculated in the perturbed model. The result shown in (a) is corresponding to the kernel in Fig. 3(b), and the result shown in (b) is corresponding to the kernel in Fig. 4(a). Details see the text.

How serious is the nonlinear effect on traveltime delays predicted by sensitivity kernels

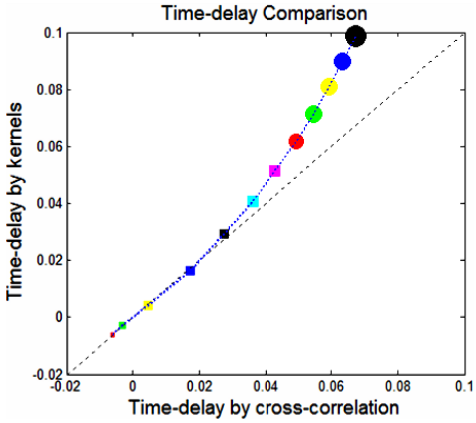

Fig.6. Comparisons between the delay times measured from synthetic seismograms and predicted by the sensitivity kernel integrals. The radius of the perturbation patch is 600 m and the velocity perturbation values are 5%, 10%, 20%, 40%, 60%, 100%, and 200% .

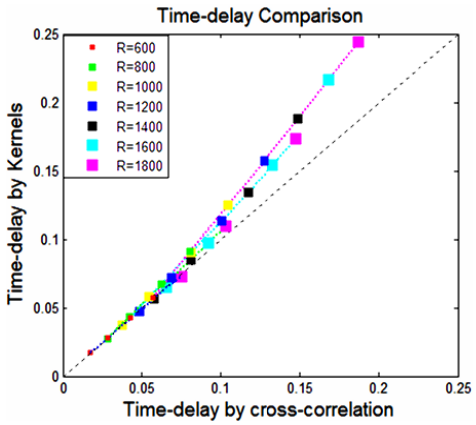

Fig.7 Comparisons between the delay times measured from synthetic seismograms and predicted by the sensitivity kernel integrals. The radii of the perturbation patchs are 600 m, 800 m, 1000 m, 1200 m, 1400 m, 1600 m and 1800 m. the velocity perturbations are 40%, 60%, 100%, and 150% . Details see text.

Conclusions

Using numerical simulations, we investigate the accuracy that the traveltime sensitivity kernel predicting the travel time delays. The predicted traveltime delays are compared to these directly measured from the synthetic seismograms and the results are used to judge the accuracy of the linear theory. Our results show that extending the scale or increasing the amplitude of the velocity perturbations or both can affect the precision of the traveltime sensitivity kernel. These factors also complicate waveforms of synthetic seismograms as well as the shape of the sensitivity kernels in the perturbed velocity model. Nevertheless, within a large range of velocity perturbations, the sensitivity kernels based on linear theory still give reasonably accurate traveltime delay, indicating the linearization plus iteration method is still effective under reasonably large velocity perturbations.

Acknowledgements

This research is supported by the WTOPI Consortium at the University of California, Santa Cruz. The facility support from the W.M. Keck Foundation is also acknowledged.

EDITED REFERENCES

Note: This reference list is a copy-edited version of the reference list submitted by the author. Reference lists for the 2009 SEG Technical Program Expanded Abstracts have been copy edited so that references provided with the online metadata for each paper will achieve a high degree of linking to cited sources that appear on the Web.

REFERENCES

Coates, R. T., and C. H. Chapman, 1990, Ray perturbation theory and the Born approximation: Geophysical Journal International, **100**, 379–392.

Dahlen, F. A., S. H. Hung, and G. Nolet, 2000, Fréchet kernels for finite-frequency traveltime: Theory: Geophysical Journal International, **141**, 157–174.

Liu, Y., and L. Dong, 2008, Sensitivity kernels and Fresnel volumes for transmitted waves: 78th Annual International Meeting, SEG, Expanded Abstracts, 3234–3238.

Luo, Y., and G. T. Schuster, 1991, Wave-equation traveltime inversion: Geophysics, **56**, 645–653.

Marquering, H., G. Nolet, and F. A. Dahlen, 1998, Three-dimensional waveform sensitivity kernels: Geophysical Journal International, **132**, 521-534.

———, 1999, Three-dimensional sensitivity kernels for finite-frequency traveltimes: The banana-doughnut paradox: Geophysical Journal International, **137**, 805–815.

Snieder, R., and C. Chapman, 1998, The reciprocity properties of geometrical spreading: Geophysical Journal International, **132**, 89–95.

Woodward, M. J., 1992, Wave-equation tomography: Geophysics, **57**, 15–26.

Xie, X. B. and H. Yang, 2008a, The finite-frequency sensitivity kernel for migration residual moveout and its applications in migration velocity analysis: Geophysics, **73**, no. 6, 241–249.

———, 2008b, A wave-equation migration velocity analysis approach based on the finite-frequency sensitivity kernel: 78th Annual International Meeting, SEG, Expanded Abstracts, 3093–3097.

Yue, T., R. Montelli, G. Nolet, and F. A. Dahlen, 2007, Computing traveltime and amplitude sensitivity kernels in finite-frequency tomography: Journal of Computational Physics, 2271–2288.